Chapter 3

Numerical Model of Single-Story Buildings equipped with a Friction Dissipator

3.1 Introduction

In this chapter an algorithm to solve the equations of motion for symmetrical, single-story buildings equipped with a friction dissipator (SSBFD) is proposed. Basically, these structures can be treated as two planar SDOF systems (the main frame and the bracing-dissipator combination). In order to formulate the equations of motion, numerical models of a friction dissipator (FD) and of the SSBFD are presented. Due to the presence of the FD, it is necessary to consider, besides the equation of motion of the bare frame —SDOF system— , the corresponding equation of motion of the FD, therefore there will be, through the entire analysis, either one or two degree-of-freedom systems, depending on the 'sliding' or 'sticking' condition between the dissipator and the main structure. This situation leads to a highly nonlinear nature of these equations. A numerical solution of this challenging problem is proposed. The energy balance equation is established.

At the final section of this chapter, some numerical examples, using the proposed algorithm and the commercial program ADINA, are presented.

3.2 Numerical Model of Friction Dissipators (FD)

As mentioned before in Chapter 1, this Thesis deals with the study of the dynamic behavior of buildings equipped with friction energy dissipation devices (simply FD). These devices are incorporated to the main structure by means of a bracing system, as shown in Fig. 1.18.

In the following, a mechanical model of a single friction dissipator is proposed. Fig. 3.1

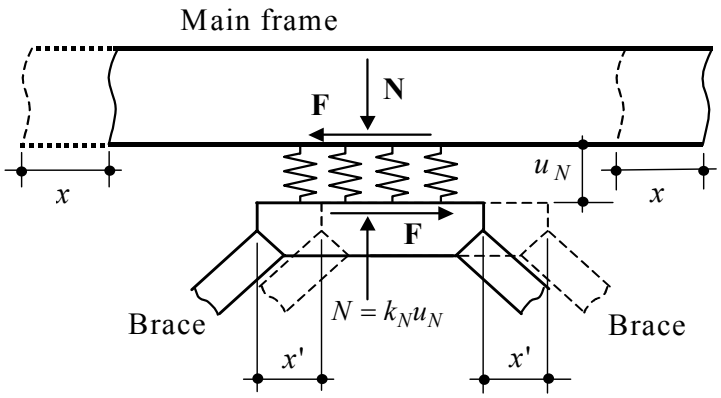

Figure 3.1 Simplified model of a friction dissipator located between the girder and the braces

shows the model and the main parameters involved in the contact analysis between the main frame and the dissipator.

In Fig. 3.1 x and x' represent, respectively, the horizontal displacements of the main frame and of the dissipation device. The coefficient k' is the stiffness of the bracing system that holds the dissipator.

In the contact surface, the limit condition for the unidirectional constitutive model —based on Coulomb's law— is

$$f(F, u_N) = g(F, u_N) = |F| - \mu N = |F| - \mu K_N \, u_N \leq 0 \tag{3.1}$$

where $f(F, u_N)$ and $g(F, u_N)$ are the plastic yielding limit function and the plastic potential, respectively [57]. F is the friction force between the dissipator and the structure, μ is the coefficient of static dry friction ($\mu = \tan \phi^{fric}$ where ϕ^{fric} is the roughness angle) and N is the pressure —acts normally to the contact surface— given by $N = K_N \, u_N$ where K_N and u_N are the penetration stiffness and the penetration displacement, respectively.

If during the calculation process the condition (3.1) is not satisfied, i.e., if $|F| > \mu N$, it means that there is sliding ($\dot{x} \neq \dot{x}'$).

3.3 Numerical Model of a SSBFD

3.3.1 Simplified model

Fig. 3.2a shows a typical single-story building equipped with a friction dissipator (SSBFD). When the structure of Fig. 3.2a is subjected to the lateral load $P(t)$ and/or to the ground motion $\ddot{x}_g$, the assumed motion of both the main frame and the friction dissipator will be as shown in Fig. 3.2b. The coordinates x and x' are the horizontal displacements of the

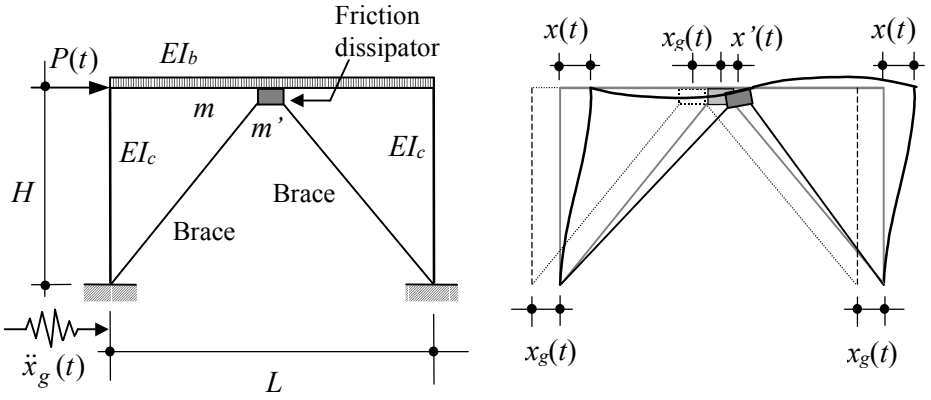

(a) Single-story building with a friction dissipator (SSBFD)

(b) Assumed motions of the main structure and the friction dissipator

Figure 3.2 Single-story building equipped with a friction dissipator (SSBFD)

main frame and of the dissipator, respectively, relative to the base (ground). The sliding displacement is, at any instant, equal to $x - x'$.

In Fig. 3.2b the dashed line represents the original position of the structure, the grey line represents the assumed undeformed new position of the structure, and the solid line represents the 'real' deformed structure.

3.3.2 Mechanical model

In order to write down the equations of horizontal motion of the SSBFD depicted in Fig. 3.2a its mechanical model is shown in Fig. 3.3a, while Fig. 3.3b shows the free-body diagram of the blocks corresponding to the main structure and to the dissipator.

3.3.3 Equations of motion of SSBFD

Considering the free-body diagrams of Fig. 3.3b, the equations of motion of the SSBFD depicted in Fig. 3.2a are

$$m\ddot{x} + c\dot{x} + kx = -m\ddot{x}_g(t) + P(t) - F \tag{3.2a}$$

$$m'\ddot{x}' + c'\dot{x}' + k'x' = -m'\ddot{x}_g(t) + F \tag{3.2b}$$

where m, c and k are the mass, the damping and the stiffness of the main structure —lower block in Fig. 3.3a—; while m', c' and k' are the mass, the damping and the stiffness of the bracing-dissipator combination —upper block in Fig. 3.3a.

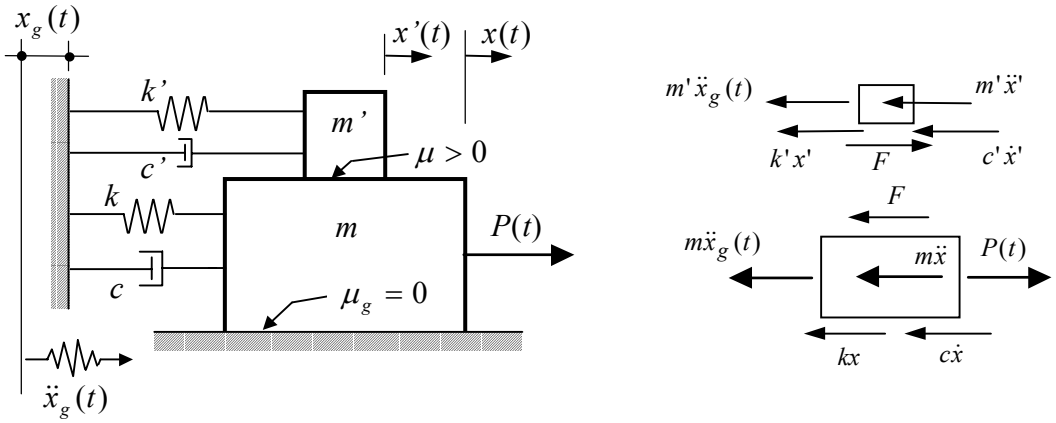

(a) Mecanical model of a single-story building with a friction dissipator (SSBFD)

(b) Free-body diagram of a SSBFD

Figure 3.3 Mechanical model of the SSBFD shown in Fig. 3.2a

Eqs. (3.2a) and (3.2b) show that the structure and the bracing system are assumed to remain elastic while the nonlinearities are concentrated in the dissipator.

For the particular structure depicted in Fig. 3.2a the stiffness k' can be obtained by means of the expression

$$k' = \frac{2EAL^2}{(4H^2 + L^2)^{3/2}} \tag{3.3}$$

where E is the Young's modulus, A is the brace cross section (only the brace under tension is considered, i.e., the brace under compression buckles), H is the column height and L is the girder length.

As described previously, x, $\dot{x}$ and $\ddot{x}$ represent the displacement relative to the ground, the velocity and the acceleration of mass m, respectively, while x', $\dot{x}'$ and $\ddot{x}'$ are the corresponding quantities for the bracing-dissipator combination. $P(t)$ is the external force acting on m, $\ddot{x}_g(t)$ is the ground acceleration, F is the friction force between the dissipation system and the main structure and t represents the time.

In the following analysis, the coefficient of friction μ_g between the ground and mass m (see Fig. 3.3a), is assumed to be zero. Due to friction terms $-F$ and $+F$, Eqs. (3.2a) and (3.2b) are nonlinear and coupled.

Eqs. (3.2a) and (3.2b) can be expressed in the following matrix form

$$\mathbf{M}\ddot{\mathbf{x}} + \mathbf{C}\dot{\mathbf{x}} + \mathbf{K}\mathbf{x} = -\mathbf{M}\mathbf{r}\ddot{x}_g(t) + \mathbf{P}(t) + \mathbf{F} \tag{3.4}$$

where

$$\mathbf{M} = \begin{bmatrix} m & 0 \\ 0 & m' \end{bmatrix} = \text{mass matrix}$$

$$\mathbf{C} = \begin{bmatrix} c & 0 \\ 0 & c' \end{bmatrix} = \text{damping matrix}$$

$$\mathbf{K} = \begin{bmatrix} k & 0 \\ 0 & k' \end{bmatrix} = \text{stiffness matrix}$$

$$\mathbf{x} = \begin{bmatrix} x \\ x' \end{bmatrix} = \text{displacement vector}$$

$$\mathbf{r} = \begin{bmatrix} 1 \\ 1 \end{bmatrix} = \text{unit vector}$$

$$\mathbf{P}(t) = \begin{bmatrix} P(t) \\ 0 \end{bmatrix} = \text{external driving force vector}$$

$$\mathbf{F} = \begin{bmatrix} -F \\ F \end{bmatrix} = \text{friction force vector}$$

Eq. (3.4) is the equivalent form of Eq. (C.3) of Appendix C. The following equivalence relationships apply: $\mathbf{Q}(\mathbf{x}, \dot{\mathbf{x}}) = \mathbf{C}\dot{\mathbf{x}} + \mathbf{K}\mathbf{x}$, $\mathbf{R} = -\mathbf{M}\mathbf{r}\ddot{x}_g + \mathbf{P}$, $\mathbf{G}^T\boldsymbol{\lambda} = -\mathbf{F}$. The solution of Eq. (C.3) by means of Lagrange multipliers is described in Appendix C.

3.4 Proposed Solution of the Equations of Motion

3.4.1 Step-by-step algorithm

Some procedures have been proposed to solve numerically the coupled equations (3.2a) and (3.2b) [58, 59]. In this work an algorithm based on the *linear acceleration method*— Newmark's method [48, 60, 61]— is developed for this purpose.

The algorithm proposed and used to solve Eqs. (3.2a) and (3.2b) is described next. This procedure is generalized in the next chapter to simulate the dynamic behavior of multi-story buildings equipped with friction dissipators. A deeper description involving stability and accuracy and computational efficiency is presented there.

INITIAL INSTANT $t_1 = 0$

At the first instant $t_1 = 0$ displacements $x(0)$, $x'(0)$ and velocities $\dot{x}(0)$, $\dot{x}'(0)$ are known. There are two possibilities:

1. If $\dot{x}(0) = \dot{x}'(0)$, there is sticking, hence Eqs. (3.2a) and 3.2b) can be added to obtain

$$\left(m + m'\right)\ddot{x}(0) + (c + c')\dot{x}(0) + kx(0) + k'x'(0) = -(m + m')\ddot{x}_g(0) + P(0) \tag{3.5}$$

The acceleration $\ddot{x}(0) = \ddot{x}(0)$ can be obtained from Eq. (3.5) and the friction force $F(0)$ is found from Eq. (3.2a) or (3.2b). If $|F(0)| \geq \mu N$, $F(0)$ is set equal to μN if $F(0) \geq \mu N$, or equal to $-\mu N$ if $F(0) < -\mu N$. A sliding condition has to be considered for next instant t_2.

2. If $\dot{x}(0) \neq \dot{x}'(0)$, there is sliding, hence the initial friction force $F(0)$ can be calculated with the following expression:

$$F(0) = \text{sgn}\left[\dot{x}(0) - \dot{x}'(0)\right]\mu N \tag{3.6}$$

and the initial accelerations $\ddot{x}(0)$ and $\ddot{x}'(0)$ can be calculated from any of the following equations:

$$m\ddot{x}(0) + c\dot{x}(0) + kx(0) = -m\ddot{x}_g(0) + P(0) - \text{sgn}\left[\dot{x}(0) - \dot{x}'(0)\right]\mu N \tag{3.7}$$

$$m'\ddot{x}'(0) + c'\dot{x}'(0) + k'x'(0) = -m'\ddot{x}_g(0) + \text{sgn}\left[\dot{x}(0) - \dot{x}'(0)\right]\mu N \tag{3.8}$$

ANY INSTANT t_{k+1}

At any instant $k + 1$, Eqs. (3.2a) and (3.2b) become

$$m\ddot{x}_{k+1} + c\dot{x}_{k+1} + kx_{k+1} = -m\ddot{x}_g(t_{k+1}) + P(t_{k+1}) - F_{k+1} \tag{3.9}$$

$$m'\ddot{x}'_{k+1} + c'\dot{x}'_{k+1} + k'x'_{k+1} = -m'\ddot{x}_g(t_{k+1}) + F_{k+1} \tag{3.10}$$

1. If at previous instant k there was sticking, this same condition is assumed at current instant $k + 1$, therefore $\dot{x}_{k+1} = \dot{x}'_{k+1}$, $\ddot{x}_{k+1} = \ddot{x}'_{k+1}$, $x_{k+1} - x'_{k+1} = x_k - x'_k$ and the entire structure can be described as a SDOF system. Its equation of motion is obtained by adding Eqs. (3.9) and (3.10):

$$\begin{aligned}\left(m + m'\right)\ddot{x}_{k+1} + (c + c')\dot{x}_{k+1} + (k + k')x_{k+1} = &-(m + m')\ddot{x}_g(t_{k+1}) \\ &+ P(t_{k+1}) + k'(x_k - x'_k)\end{aligned} \tag{3.11}$$

The displacement x_{k+1} and velocity $\dot{x}_{k+1}$ are obtained from Eq. (3.11) using Newmark's method, as described in Appendix B. The friction force F_{k+1} can be calculated afterwards using Eq. (3.9) or (3.10).

   (a) If $|F_{k+1}| < \mu N$, the sticking condition keeps for next instant $k + 2$.

(b) If $|F_{k+1}| \geq \mu N$, the sticking condition no longer prevails for next instant $k+2$. Since the maximum absolute value of the friction force is limited to μN, F_{k+1} is either set equal to μN if $F_{k+1} \geq \mu N$, or to $-\mu N$ if $F_{k+1} < -\mu N$. For instant $k+2$ the sliding condition will be assumed.

2. If at previous instant k there was sliding, this same condition is assumed at current instant $k+1$, i.e., $F_{k+1} = F_k = \text{sgn}(\dot{x}_k - \dot{x}'_k)\,\mu N$. In this case there are two uncoupled SDOF systems described by the following equations of motion:

$$m\ddot{x}_{k+1} + c\dot{x}_{k+1} + kx_{k+1} = -m\ddot{x}_g(t_{k+1}) + P(t_{k+1}) - \text{sgn}\left(\dot{x}_k - \dot{x}'_k\right)\mu N \tag{3.12}$$

$$m'\ddot{x}'_{k+1} + c'\dot{x}'_{k+1} + k'x'_{k+1} = -m'\ddot{x}_g(t_{k+1}) + \text{sgn}\left(\dot{x}_k - \dot{x}'_k\right)\mu N \tag{3.13}$$

Eqs. (3.12) and (3.13) are solved using Newmark's method (see Appendix B).

The sliding condition keeps as long as the sign of the relative velocity $\dot{x} - \dot{x}'$ remains the same:

(a) If $(\dot{x}_k - \dot{x}'_k)\left(\dot{x}_{k+1} - \dot{x}'_{k+1}\right) > 0$, the sliding condition prevails for next instant $k+2$.

(b) If $(\dot{x}_k - \dot{x}'_k)\left(\dot{x}_{k+1} - \dot{x}'_{k+1}\right) \leq 0$, the sliding condition no longer keeps for the next instant $k+2$ (i.e., a sticking condition will be assumed at instant $k+2$).

As pointed out in the above procedure, the same sticking-sliding condition keeps for at least two consecutive time steps. In this way, the response tends to be smoother.

This algorithm is represented schematically in the flow-chart of Fig. 3.4.

In Section 3.6 the preceding procedure will be applied to solve some practical cases.

3.5 Energy Balance Relations

If Eq. (3.4) is pre-multiplied and post-multiplied by $\dot{\mathbf{x}}^T = [\dot{x},\ \dot{x}']$ and dt, respectively, and then integrated through time, the following equation is obtained

$$E_K + E_D + E_S = E_I - E_F \tag{3.14}$$

where

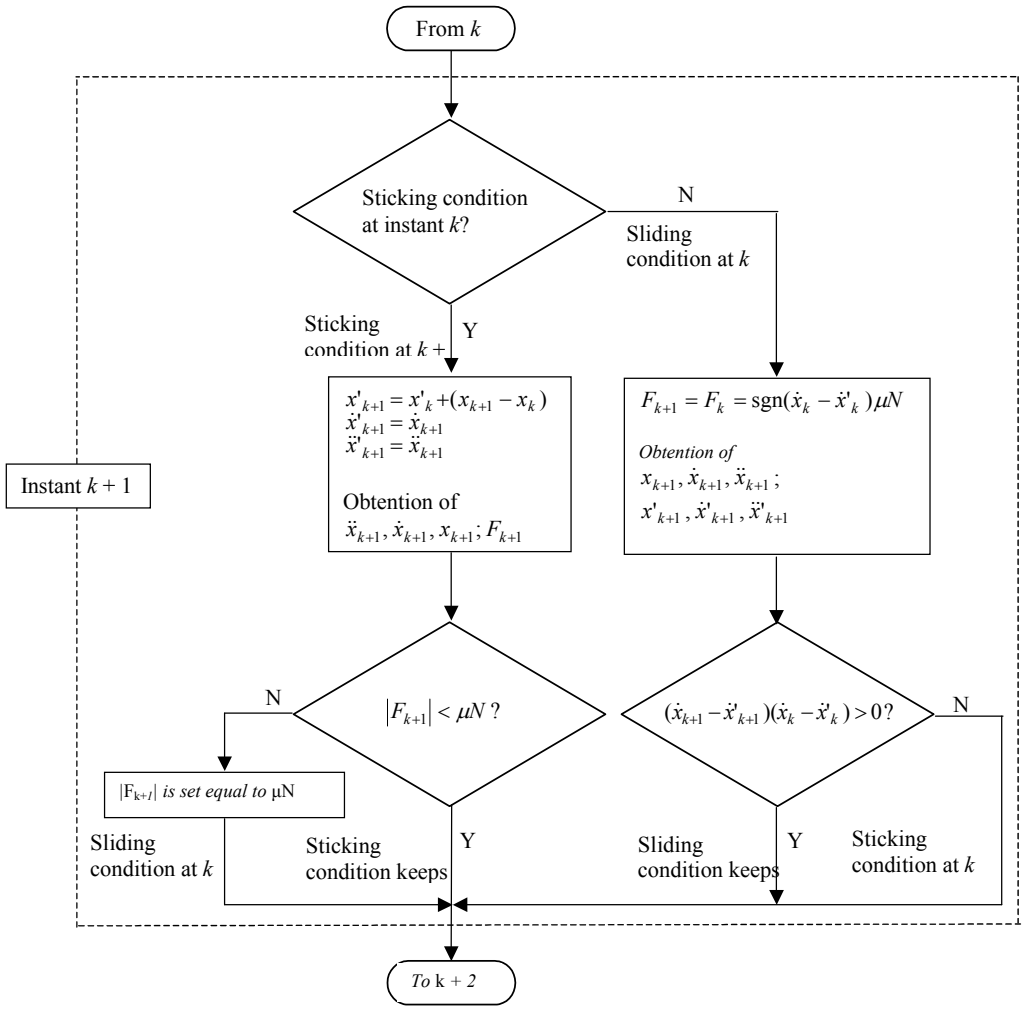

Figure 3.4 Flowchart that shows the proposed solution of the equations of motion of SSBFD

$$
\begin{aligned}
E_K &= \int_0^t m\ddot{x}\dot{x}dt + \int_0^t m'\ddot{x}'\dot{x}'dt = \frac{1}{2}m(\dot{x}^2 - \dot{x}(0)^2) + \frac{1}{2}m'(\dot{x}'^2 - \dot{x}'(0)^2) \\
E_D &= \int_0^t c\dot{x}\dot{x}dt + \int_0^t c'\dot{x}'\dot{x}'dt = \int_0^t c\dot{x}^2dt + \int_0^t c'\dot{x}'^2dt \\
E_S &= \int_0^t kx\dot{x}dt + \int_0^t k'x'\dot{x}'dt = \frac{1}{2}k(x^2 - x(0)^2) + \frac{1}{2}k'(x'^2 - x'(0)^2) \\
E_I &= -\int_0^t m\ddot{x}_g\dot{x}dt - \int_0^t m'\ddot{x}_g\dot{x}'dt + \int_0^t P\dot{x}dt = -\int_{x(0)}^{x} m\ddot{x}_g dx \\
&\qquad\qquad - \int_{x'(0)}^{x'} m'\ddot{x}_g dx' + \int_{x(0)}^{x} Pdx \\
E_F &= \int_0^t F\dot{x}dt - \int_0^t F\dot{x}'dt = \int_{x(0)}^{x} Fdx - \int_{x'(0)}^{x'} Fdx'
\end{aligned}
\tag{3.15}
$$

The terms included in the left member of Eq. (3.14) represent the kinetic energy (E_K) of the entire structure, the energy dissipated by means of the viscous damping (E_D) of the entire structure and the strain energy (E_S). The addition of these terms must be equal to the input energy introduced to the structure (E_I) due to any lateral force minus the energy dissipated by friction (E_F).

Eqs. (3.15) are useful to determine the values of the time-history energies of a particular SSBFD subjected to any driving force.

3.6 Numerical Examples

3.6.1 Structure description

Basically, the SSBFD is the one depicted in Fig. 3.2a and shown again in Fig. 3.5. The dynamic properties of the structure are registered in Table 3.1. The main structure stiffness, k, was calculated using Eq. (B.3) with $E = 200$ GPa, $I_b \to \infty$, $I_c = 576$ cm^4, $H = 480$ cm, $L = 800$ cm; and the brace stiffness (tension only) k' was calculated using Eq. (3.3) with $A = 1.98$ cm^2.

3.6.2 Free vibration

For an initial displacement of 10 cm ($x(0) = x'(0) = 10$ cm; $\dot{x}(0) = \dot{x}'(0) = 0$; $P(t) = 0$ and $\ddot{x}_g(t) = 0$), the dynamic response for the frame of Fig. 3.5 will be obtained.

The sliding threshold, μN, is set equal to 39.325 kN. The time increment is $\Delta t = 0.00115$ s and the total duration of the analysis is 0.55 s.

The frame and the dissipator displacement responses are depicted in Fig. 3.6. The thick black line corresponds to the main frame displacement and the thin black line corresponds

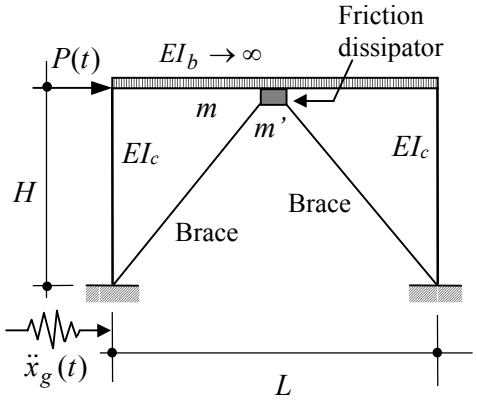

Figure 3.5 Single-story building with a friction dissipator (SSBFD)

Main structure	**Bracing system + dissipator**
$m = 5740.390$ kg	$m' = 19.614$ kg
$c = 13121.77$ N·s/m ($\xi = 0.05$)	$c' = 0.0$ ($\xi' = 0.0$)
$k = 2999.471$ kN/m	$k' = 2597.01$ kN/m
$T = 0.2749$ s	

Table 3.1 Structure and bracing + dissipator data

to the dissipator displacement, respectively. The upper and lower horizontal grey lines correspond to the thresholds $\mu N/k'$and $-\mu N/k'$, respectively. These values limit the displacement of the dissipator (see Fig. B5 in Appendix B). The smaller the values of m', the lesser the oscillation amplitudes of x' around these thresholds (see Eq. (3.2b)).

Fig. 3.7 shows a plot of $F - (x - x')$. This is actually a plot of the theoretical hysteresis loops due to the sticking-sliding behavior of the friction dissipator. The shape of the hysteresis loops are rectangular, according to Coulomb's law of dry friction (see Subsect. 2.2.2).

3.6.3 Harmonic loading applied to the main structure

In this case the external input force is a harmonic loading $P(t) = P_0 \sin \bar{\omega} t$ (i.e., $\ddot{x}_g(t) = 0$). This driving force is plotted in Fig. 3.8 and will be applied to the frame of Fig. 3.5. The values of P_0 and $\bar{\omega}$ are, respectively, 127.491 kN and 15.9781 rad/s. On the other hand, the values of m, c, k and m', c', k' are the same shown in Table 3.1. The values of μN and Δt are also the same as before. However, in this case the total duration of this driving force is 1.18 s.

The displacement responses of the frame and of the dissipator are shown in Fig. 3.9. The thick black line corresponds to the main frame displacement and the thin black line

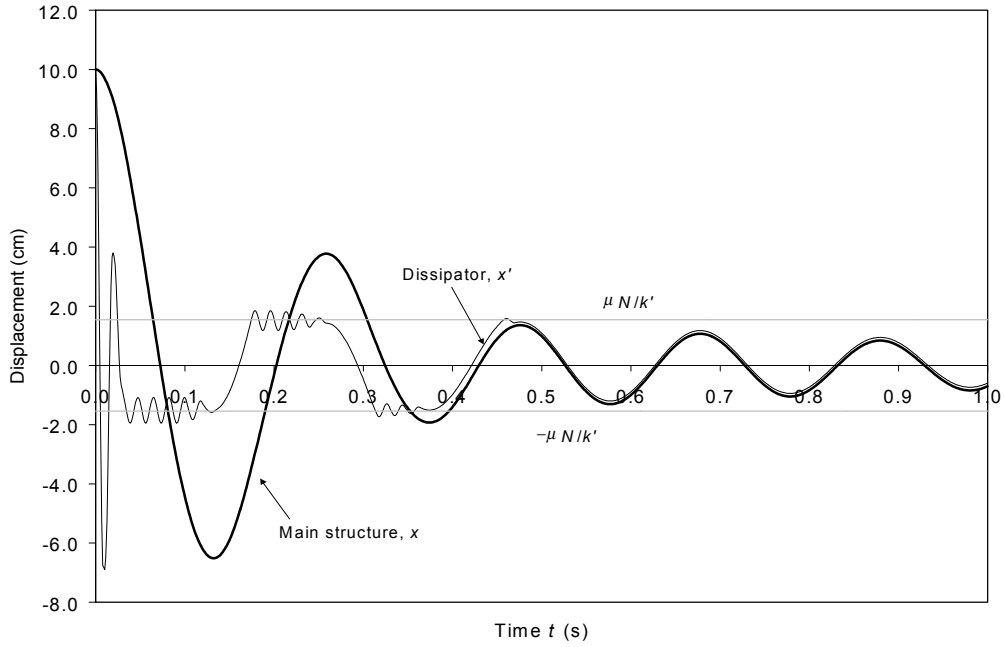

Figure 3.6 Displacement response of a SSBFD subjected to an initial displacement

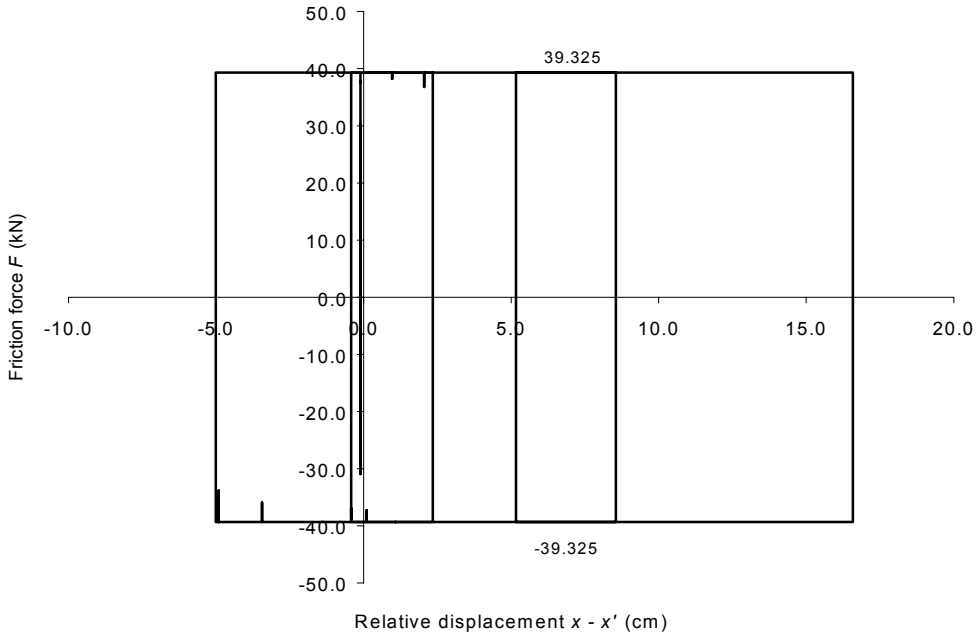

Figure 3.7 $F-(x-x')$ relationship of a SSBFD subjected to an initial displacement

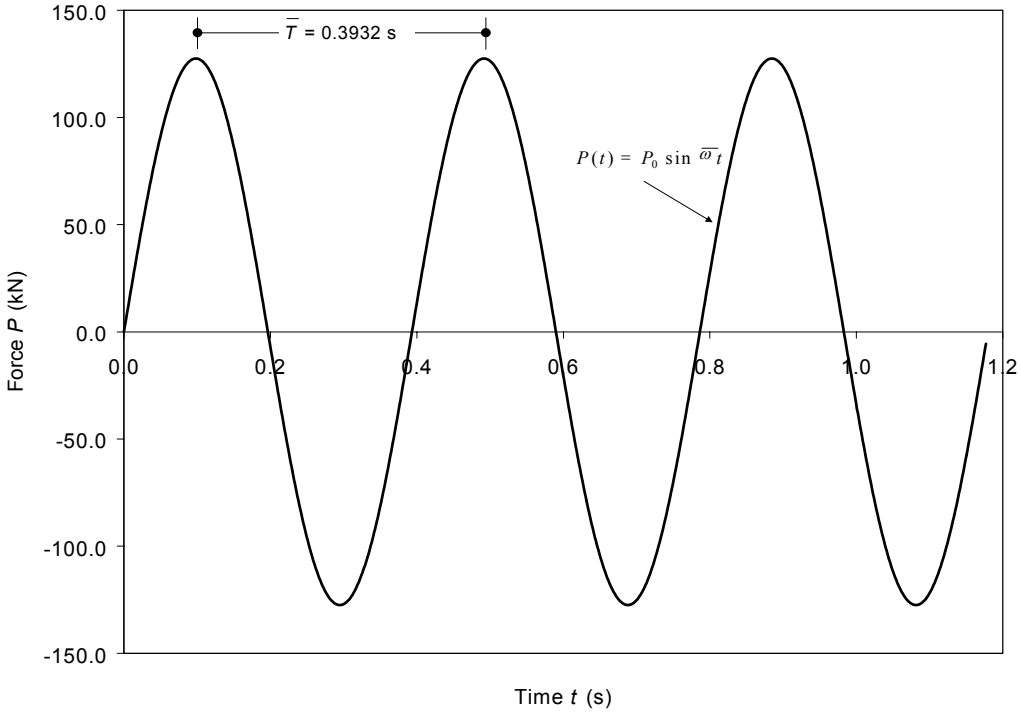

Figure 3.8 Harmonic loading to be applied to the frame of Fig. 3.5

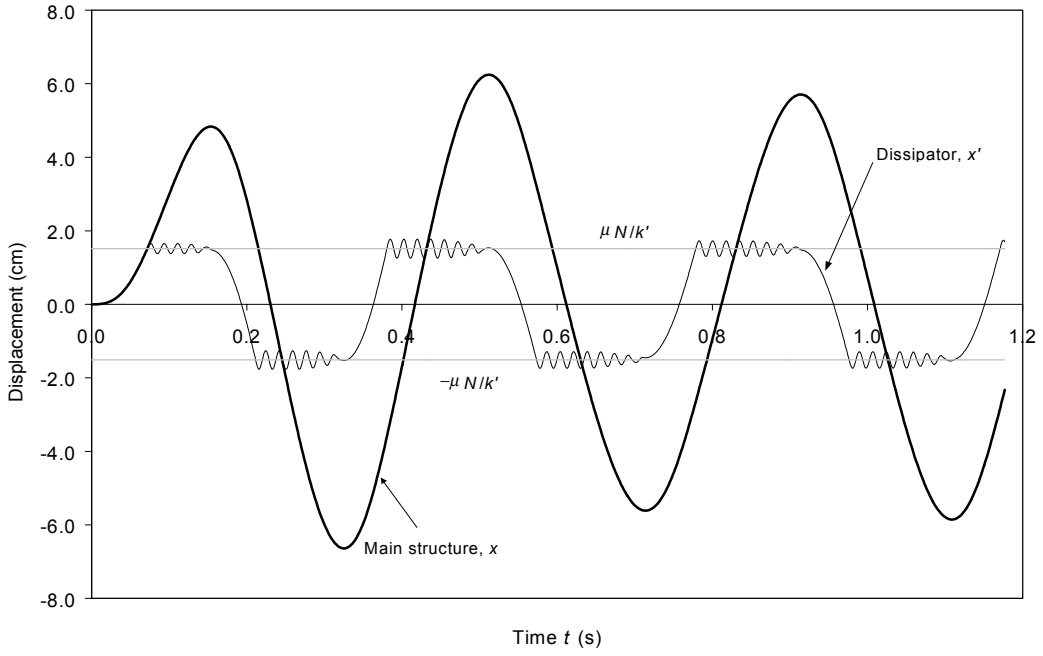

Figure 3.9 Displacement response of a SSBFD subjected to a harmonic loading

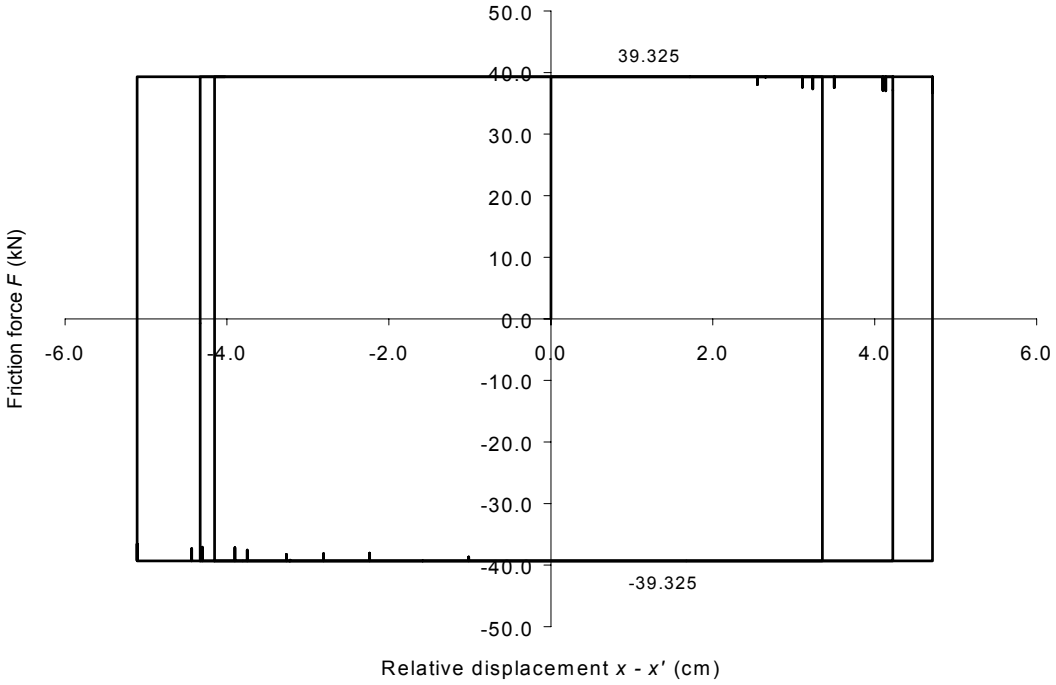

Figure 3.10 $F-(x-x')$ relationship of a SSBFD subjected to a harmonic loading

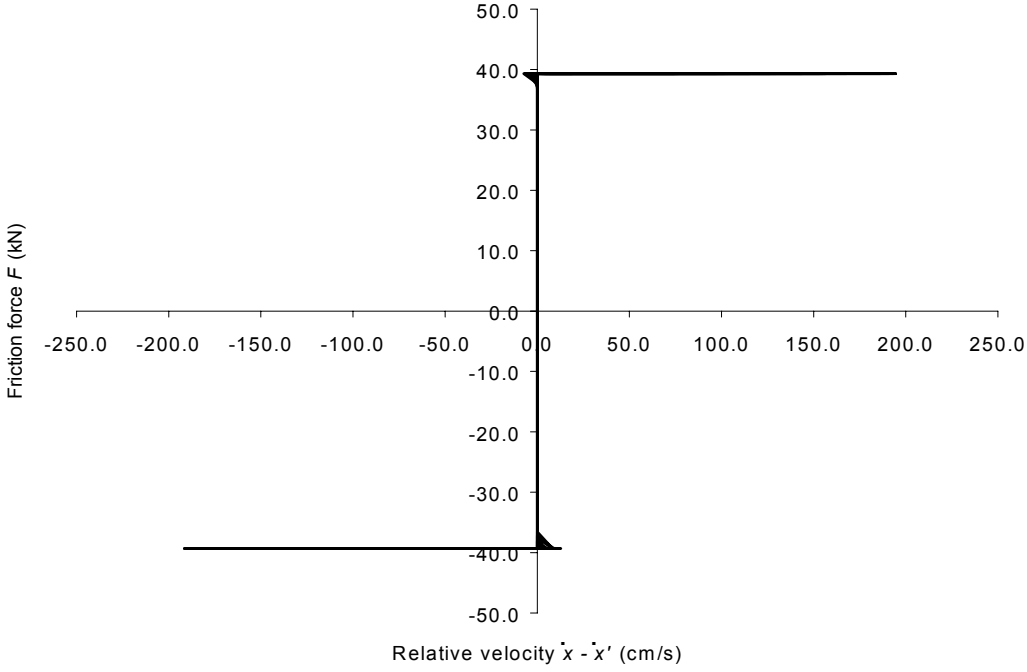

Figure 3.11 $F-(\dot{x}-\dot{x}')$ relationship of a SSBFD subjected to a harmonic loading

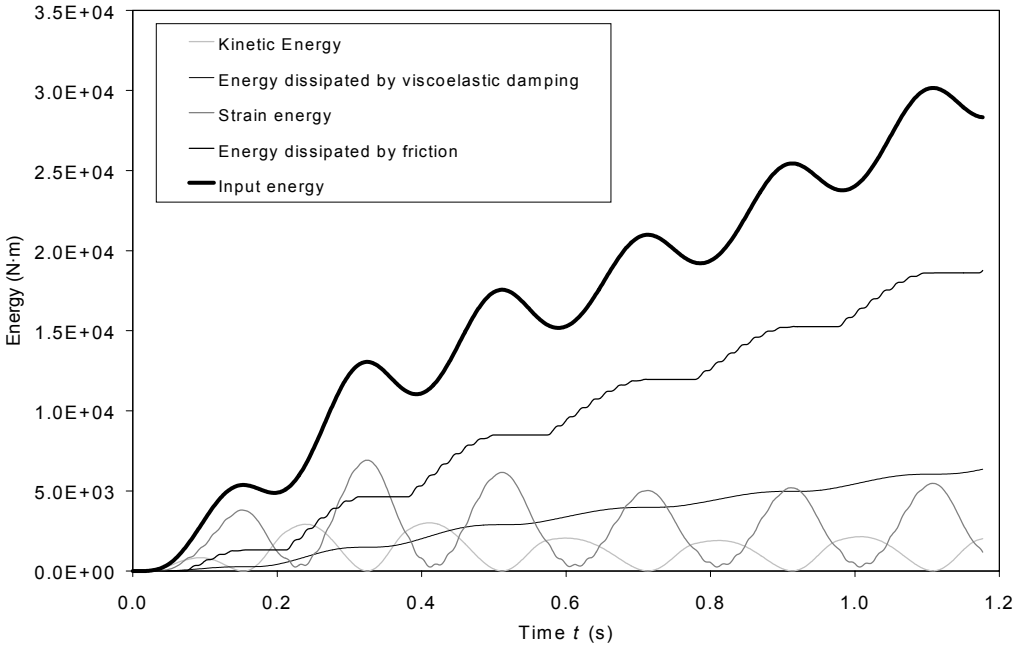

Figure 3.12 Energy response of a SSBFD subjected to a harmonic loading

corresponds to the dissipator displacement. In this figure the horizontal grey lines that restrain the dissipator displacement, as in Fig. 3.6, are depicted too.

Fig. 3.7 shows the plot of $F-(x-x')$ for this case. As said above, the shape of the hysteresis loops are rectangular, according to Coulomb's law of dry friction.

Also for this case, a plot of $F-(\dot{x}-\dot{x}')$ is shown in Fig. 3.11. It can be seen easily that the shape of this plot fits the theoretical one shown in the theory of Appendix A (see Fig. A.3). Around the corner, however, there are some 'bevels' that result from the inaccuracies of the numerical solution.

The energy time-histories are plotted in Fig. 3.12. The values of each curve were calculated with Eqs. (3.15). The line corresponding to the energy dissipated by friction is very close to the curve of the input energy, which gives an idea of the energy dissipated by friction (see the energy balance equation (3.14)).

3.6.4 Seismic input

The accelerogram corresponding to the Northridge earthquake (Santa Monica station, January 17, 1990, 90° component) is shown in Fig. 3.13. This ground acceleration, scaled by a factor of 5.0, is going to be applied to the frame of Fig. 3.5 ($P(t)=0$). Once more, the values of m, c, k and m', c', k' are the same previously given (see Table 3.1). However, in this case $\mu N = 78.456$ kN, a time increment of 0.00125 s was used and the total time of

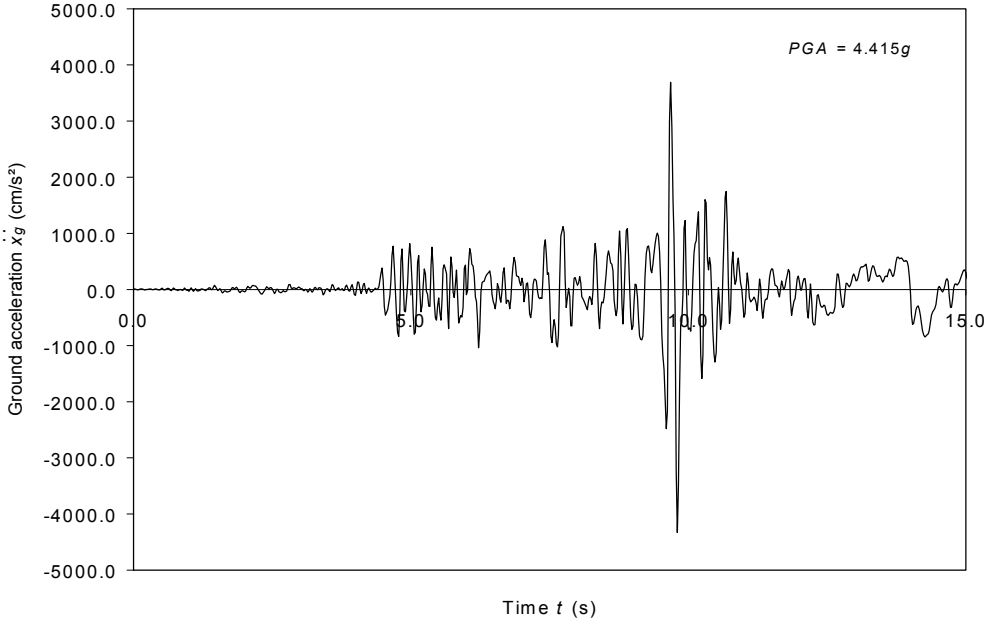

Figure 3.13 Northridge earthquake, January 17, 1994 (90° component)

analysis is 15 s. Since the accelerogram ordinates were scaled by a factor of 5.0, the PGA is equal to $4.415g$ ($g = 980.7$ cm/s^2).

Fig. 3.14 shows a plot of $F - (x - x')$.

The energy time-histories for the SSBFD, calculated with Eq. (3.15) are shown in Fig. 3.15. Again, the energy dissipated by friction lies just down the line showing the total input energy due to the earthquake.

3.7 Comparison between the Proposed Algorithm and ADINA

The practical cases seen in the prior section, were solved with the ADINA program too. The responses of the main structure have been plotted for the three cases above studied. In Fig. 3.16 the displacement response of Fig 3.6 plus the displacement response of the same structure obtained using ADINA are compared. On the other hand, in Fig. 3.17 the response of Fig. 3.9 and the response of the same structure obtained with ADINA are plotted. Finally, Fig. 3.18 shows the response of Fig. 3.13 obtained with the proposed algorithm, and the response of the same structure obtained with ADINA. The agreement is satisfactory.

The proposed algorithm has been tested with more examples using both different structure properties and different driving forces (including impulse loadings, harmonic loadings

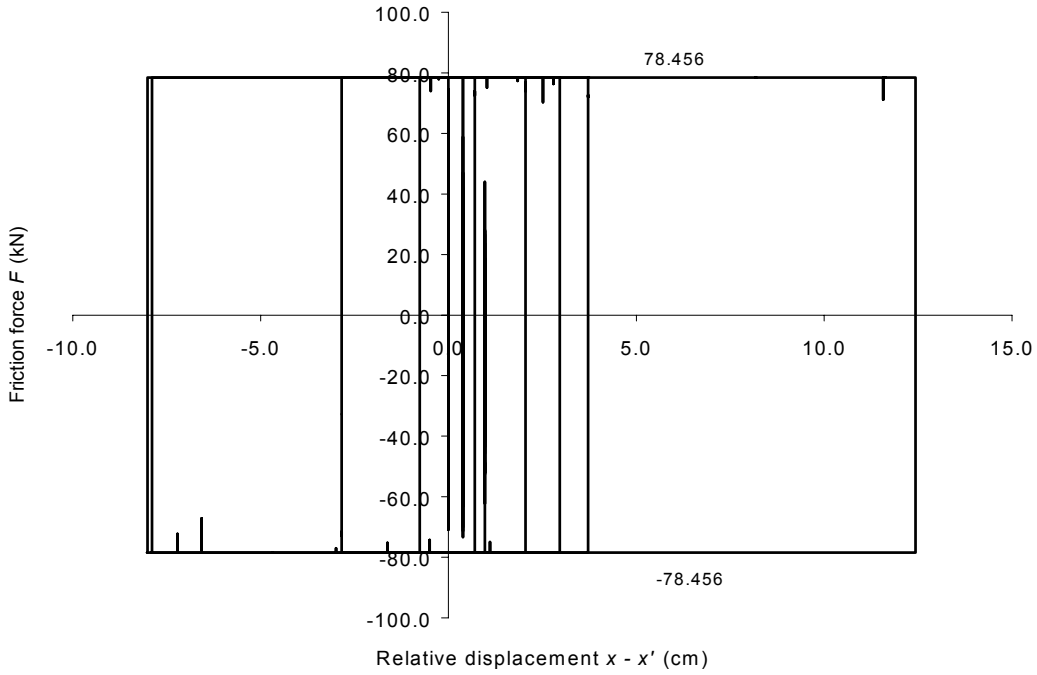

Figure 3.14 $F-(x-x')$ relationship of a SSBFD subjected to a ground acceleration

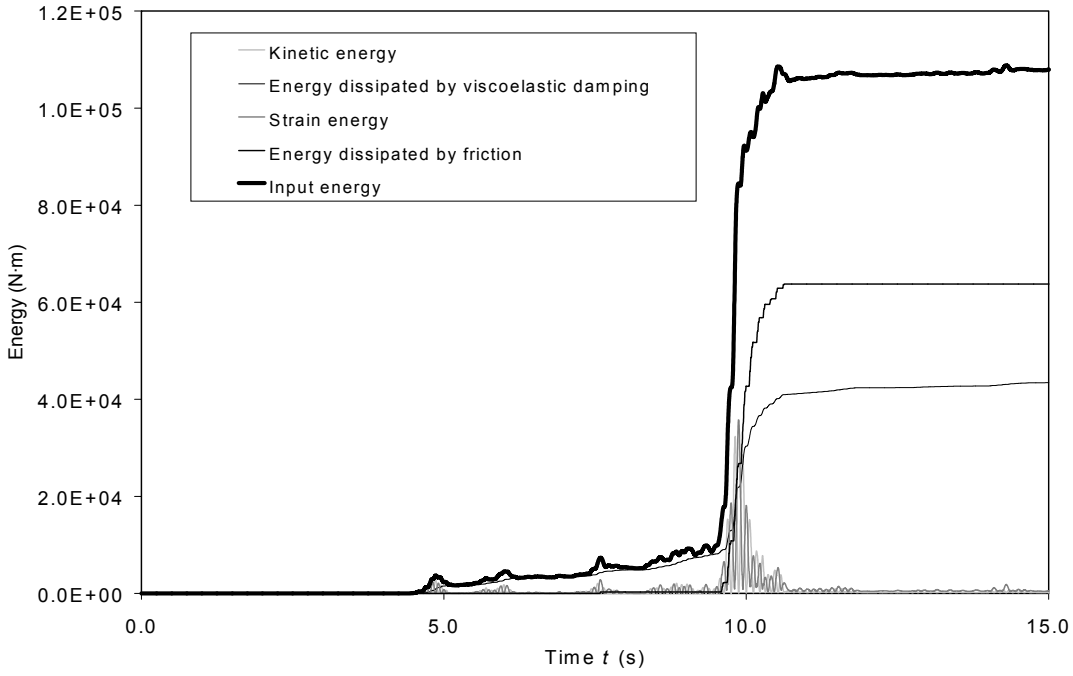

Figure 3.15 Energy response of a SSBFD for a ground acceleration

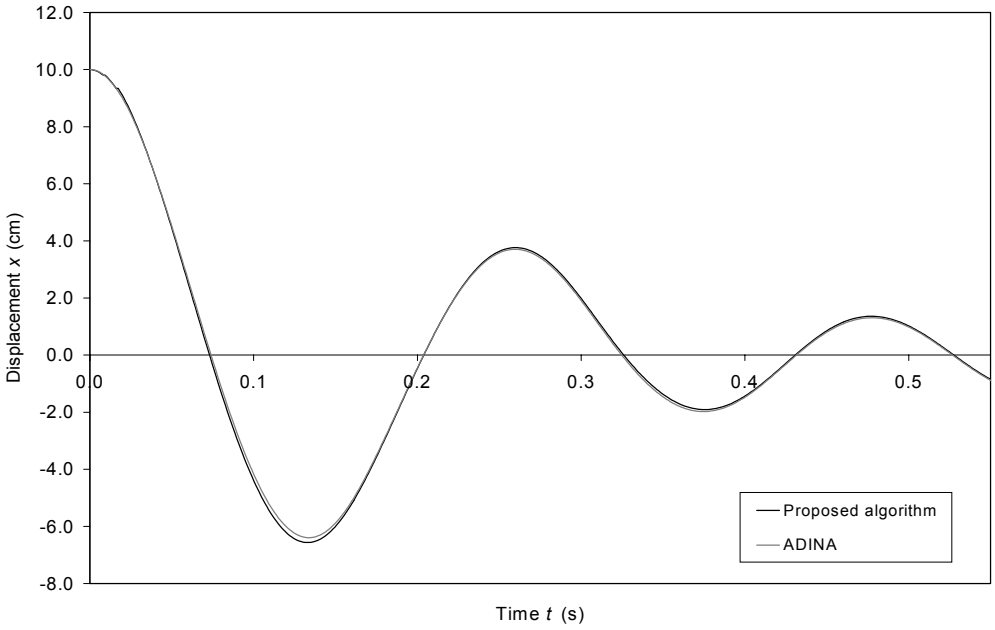

Figure 3.16 Displacement responses obtained with the proposed algorithm and ADINA for an initial displacement

and other registered earthquakes). The results obtained are practically the same given by ADINA. This evidence does not necessarily mean that the proposed algorithm is accurate, rather it means that using different approaches to those considered in the Lagrange multipliers (see Appendix C), the problems involving contact problems can be solved using direct-time integration procedures, as in the proposed algorithm.

3.8 Efficiency of Friction Dissipators

The reduction of the displacement response is highlighted in Figs. 3.19, 3.20 and 3.21 for the three inputs above considered. The black line shows the response for the SSBFD (protected frame) and the grey line shows the response for the bare frame (SSB without dissipator nor bracing).

Fig. 3.19 shows that the period of the free response tends to shorten while there is sliding. After the final sticking, the frame behaves as a SDOF (braced frame) and, obviously, the period keeps constant.

As a preliminary conclusion, the plots of Figs. 3.19, 3.20 and 3.21 show that friction dissipators reduce the response of SSB subjected to lateral loads. Other analyses show that this reduction of response, however, is never greater than the reduction obtained if rigid connections between the main frame and the braces are used (braced frames). This fact

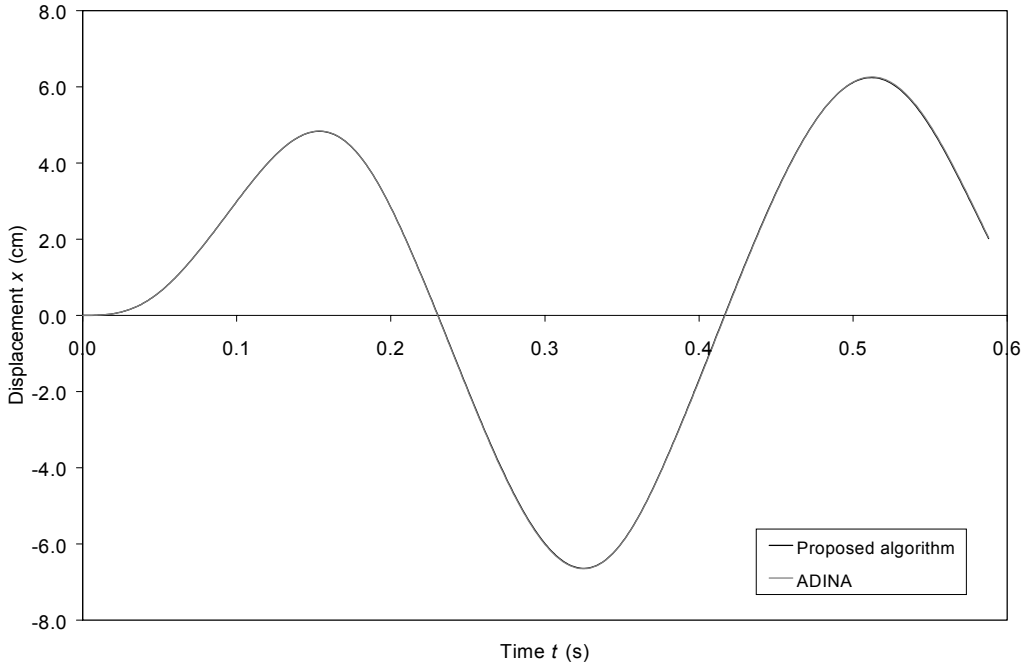

Figure 3.17 Displacement responses obtained with the proposed algorithm and ADINA for a harmonic loading

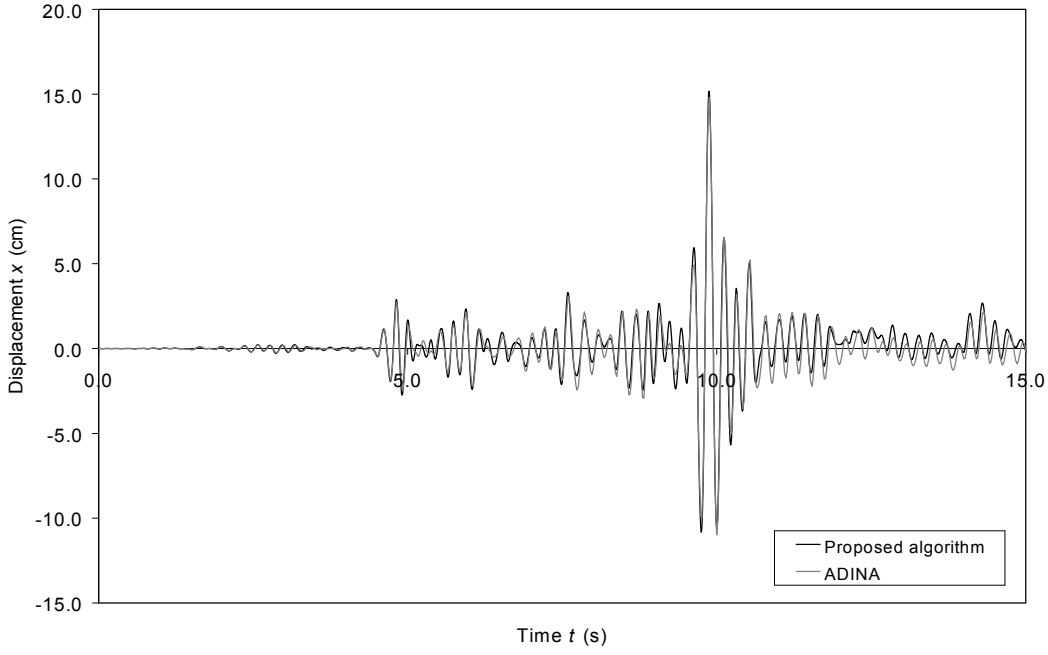

Figure 3.18 Displacement responses with the proposed algorithm and ADINA for a ground acceleration

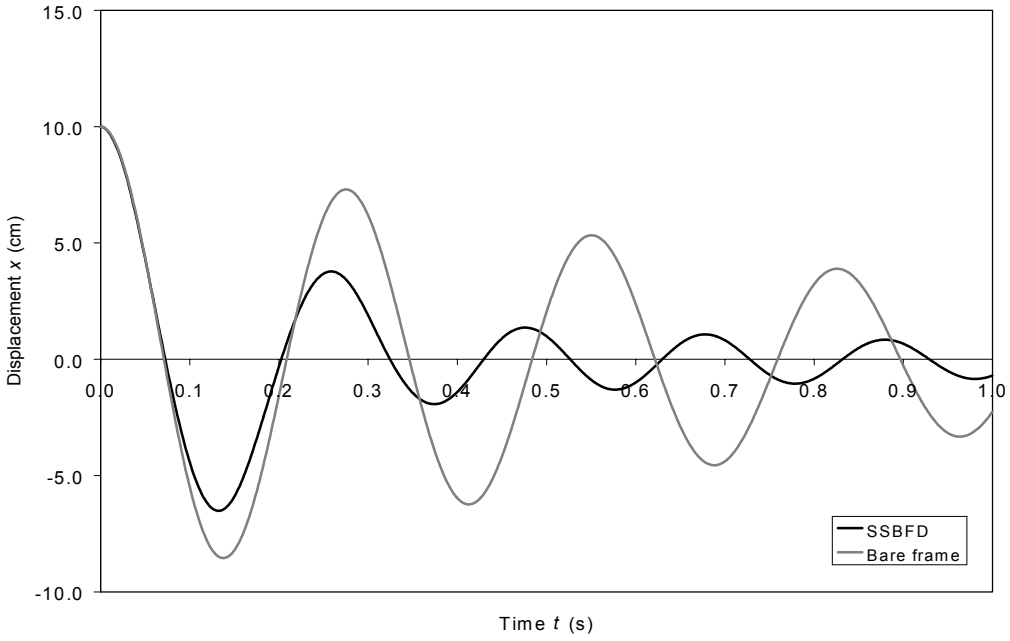

Figure 3.19 Displacement responses of the protected frame and the bare frame for an initial displacement

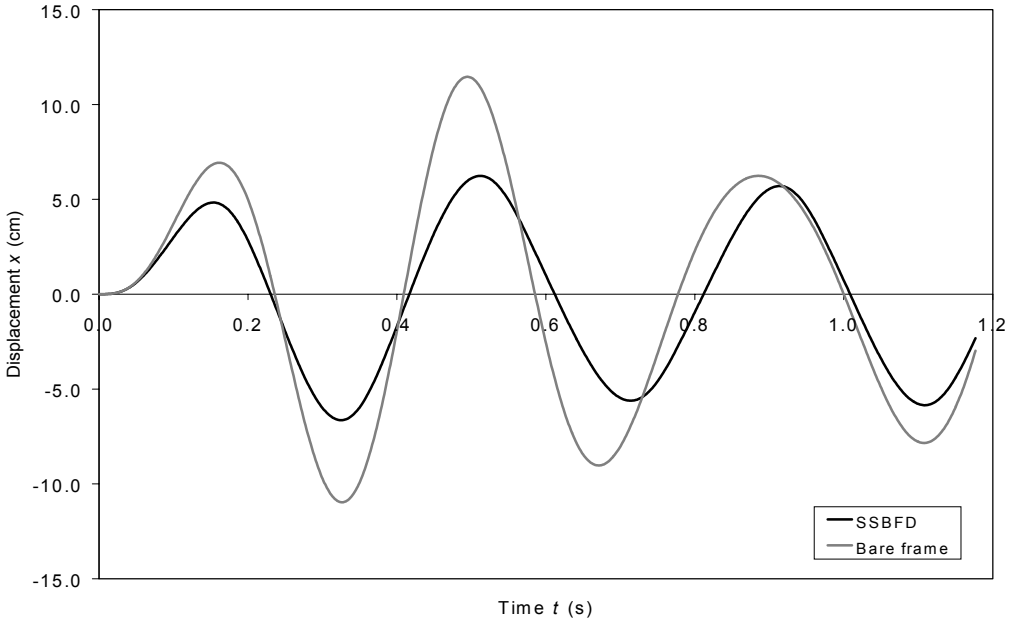

Figure 3.20 Displacement responses of a SSBFD and a bare frame for a harmonic loading

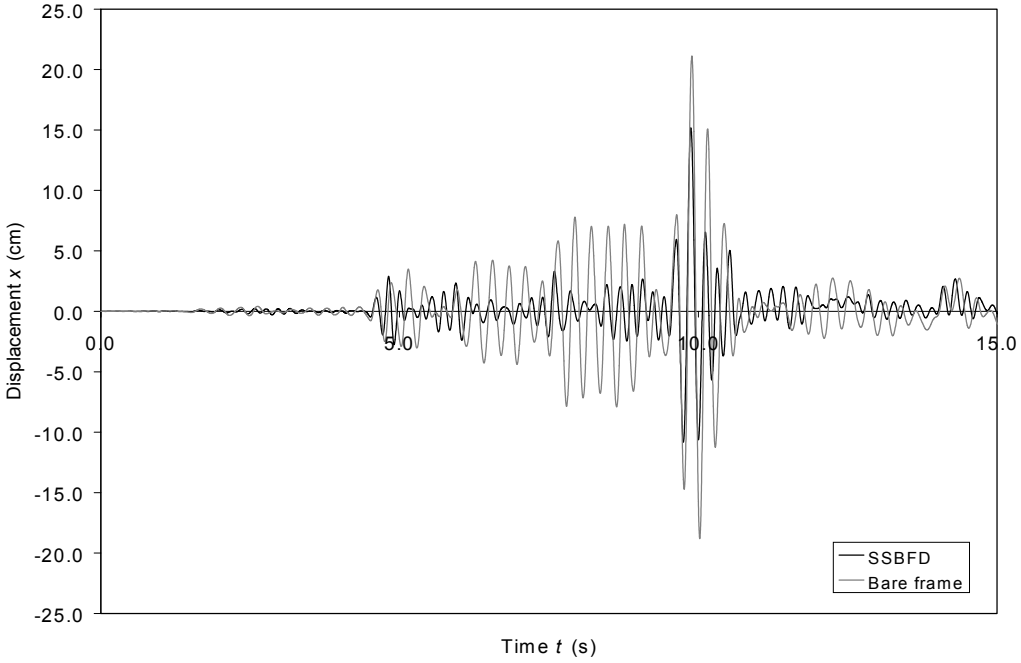

Figure 3.21 Displacement responses of a SSBFD and a bare frame for a ground acceleration

seems to confirm the conclusions stated in [52].